PCCP

Transport Characteristics of Organic Solvents through Carbon Nanotube Filled Styrene Butadiene Rubber Nanocomposites:Influence of Rubber - Filler Interaction, Degree of Reinforcement and Morphology

Journal:	*Physical Chemistry Chemical Physics*
Manuscript ID:	CP-ART-02-2015-000719.R2
Article Type:	Paper
Date Submitted by the Author:	13-Mar-2015
Complete List of Authors:	Abraham, Jiji; Mahatma Gandhi University, International and Inter University Centre for Nanoscience and nanotechnology Maria, Hanna; Mahatma Gandhi University, School of chemical sciences Kalarikkal, Nandakumar; mahatmagandhi university, International and Inter University Centre for Nanoscience and nanotechnology George, Soney; Amal Jyothi College of Engineering, Center for Nanoscience and Technology Thomas, Sabu; mahatmagandhi university, International and Inter University Centre for Nanoscience and nanotechnology

Transport Characteristics of Organic Solvents through Carbon Nanotube Filled Styrene Butadiene Rubber Nanocomposites: Influence of Rubber - Filler Interaction, Degree of Reinforcement and Morphology

Jiji Abraham[1], Hanna J Maria[1], Soney C George[2], Nandakumar Kalarikkal[1], Sabu Thomas[1*]

[1]*International and Inter University Centre for Nanoscience and Nanotechnology, Mahatma Gandhi University, P.D Hills, Kottayam, Kerala, 686560, India*

[2]*Centre for Nanoscience and Nanotechnology, Amal Jyothi College of Engineering, Kottayam, Kerala, India*

Abstract

Transport behaviour of some aromatic and aliphatic solvents through carbon nanotube filled styrene butadiene rubber composites has been investigated. The aim of the present work is to investigate the role of sorption technique in analysing the compatibility and reinforcing effect of MWCNT as filler in SBR matrix. It is also focussed to investigate the relationship between the dispersion of CNT in SBR matrix and its transport behaviour. The diffusion and transport of organic solvents through the membranes have been investigated in detail as a function of CNT content, nature of solvent and temperature in the range of 28−60 °C. Solvent uptake, diffusion, sorption and permeation constants were investigated and were found to decrease with the increase of CNT loading. Transport property could be related to the morphology of the nanocomposites. At high concentration CNT particles are forming a local filler–filler network in the rubber matrix. As a result, transport of solvent molecules through the polymer is hindered. The rubber – solvent interaction parameter, enthalpy and entropy of sorption have also been estimated from the transport data. The values of rubber –solvent interaction parameters obtained from the diffusion experiments have been used to calculate the molecular mass between crosslinks of the network polymer. The better reinforcement at higher filler loading was confirmed from the cross-link density values. The extent of reinforcement was evaluated by Kraus and Cunneen and Russel equations. The Affine and Phantom models for chemical crosslinks were used to predict the mobility of the crosslinks. The Phantom model gave better fitting indicating that the chains can move freely through one another, i.e. the junction points fluctuate over time around their mean position without any hindrance from the neighbouring molecule. The diffusivity data of the systems have shown dependence on the temperature and microstructure of nanocomposite. Finally, the diffusion data has been compared with theoretical predictions.

Key words: SBR, CNT, Nanocomposites, Diffusion, Crosslink density

1. Introduction

Polymer composites based on nano fillers have become one of the most attractive domains in the area of materials science. Among various nano fillers used, CNTs (carbon nano tubes) have got a special attention in research industry due to some of its exciting intrinsic properties. [1] [2] [3] Since their discovery by Ijima [4] they have very much attention and are now being used for many fundamental and advanced applications.

Transport of liquids through polymeric membranes is a key controlling factor in many of its applications. The transport of organic liquids through polymers is of technological importance in a variety of applications such as pervaporation, reverse osmosis and food packaging. The transport of small molecules through polymer membrane happens due to random molecular motion of individual molecules

The diffusion process is a kinetic parameter and it depends on the free volume within the matrix, nature of the polymer, crosslink density, nature of fillers, penetrant size, temperature and the degree of reinforcement. Fillers have a substantial role in the transport process. Carbon black, silica and clay are some of the frequently used fillers. If the filler is compatible with the matrix it occupies free volume within the matrix and hinders the movement of solvent through it.[5] In literature there are numerous works on the transport properties of solvents through various types of polymers including elastomers, interpenetrating networks and blends.[6] [7] [8] [9] Unnikrishnan *et al*.[10] analysed the role of nature of crosslinks on the sorption and diffusion of aromatic hydrocarbons through cross linked natural rubber. Diffusion of aromatic solvents through SBR vulcanized by different vulcanizing agents and carbon black filled SBR were reported by George *et al.*[11] [12] Thomas *et al*. studied the effect of filler geometry on the diffusion and transport behaviour of aromatic solvents and commercial oil through nitrile rubber nanocomposites.[13] Starkova *et al*. investigated the moisture uptake and swelling effect of MWCNT-based epoxy composites in a wide range of atmosphere humidity and water uptake at various temperatures.[14] Recently in our laboratory Maria *et al.* investigated the effect of clay loading on the sorption behaviour of NR/NBR blends.[15] Jose *et al.* analysed the transport properties of hybrid nanoparticle based cross linked polyethylene (XLPE)–Al_2O_3–clay binary and ternary nanocomposites.[16]

The main intention of this study is to investigate the advantages of sorption technique in analysing the compatibility and reinforcing effect of MWCNT as filler in SBR matrix. To the best of our knowledge, no studies have been reported on the diffusion behaviour of CNT through SBR rubber matrix. Styrene–butadiene rubber (SBR) is a general purpose synthetic rubber. Due to high filler-loading capacity, good flex resistance, crack-initiation resistance and abrasion resistance it is useful in several engineering and industrial applications. This work focuses on the effect of penetrant size, filler loading, nature of penetrant and temperature on the transport of solvents through SBR/CNT nanocomposite membranes. Transport parameters have been calculated for each nanocomposite and finally the effect of temperature on these parameters and network structure has been investigated. In order to correlate the morphology with the transport behaviour, the CNT dispersion has been carefully studied by transmission electron microscopy. Finally experimental results have been correlated with theoretical predictions of Peppas– Sahlin model.

2. Experimental

2.1 Materials

Styrene Butadiene rubber (Synaprene 1502) with a 25% styrene content was used for this study. MWCNT obtained from Nanocyl, Belgium was used as the filler. Solvents used in this study were Hexane, Heptane, Octane, Toluene and Xylene of AR grade obtained from Merck chemicals. All other compounding ingredients were of analytical grade. Details of materials used are given in Table1a & 1b.

Table 1a Detailed description of materials used

Material	Molecular weight (gm mol^{-1})	Density (gm cm^{-3})	Solubility parameter (Cal $cm^{-3})^{1/2}$	Others	Source
SBR	Mn = $4X10^5$	0.93	8.1-8.6	Mooney Viscosity(100^oC) 52 ML1	Apollo Tyres Chennai
MWCNT		1.4		Purity, 90% Diameter 20nm Length- 1.5um	Nanocyl, Belgium

Table 1b Detailed description of solvents used

Material	Molecular weight (gm mol^{-1})	Molar volume	Density (gm cm^{-3})	Boiling point(^0C)	Solubility parameter (cal $cm^{-3})^{1/2}$
Hexane	86.17	128.61	0.659	68	7.3
Heptane	100.21	146.50	0.684	98.42	7.4
Octane	114.23	162.48	0.703	125.7	7.54
Toluene	92.14	105.90	0.867	110.6	8.9
Xylene	106.17	123.45	0.860	138.4	8.8

2.2 Preparation of composites

Mixing of SBR and MWCNT was done in laboratory scale two roll mixing mill. The formulations of different mixes are given in Table 2. Cure properties of the compounded samples were determined using Moving Die Rheometer at a temperature 160^0 C. Samples were then moulded by using an electrically heated hydraulic press under a pressure of 120 bar at 160^0C. Samples were prepared with different CNT content and designated as ST_0, $ST_{0.5}$, ST_1, ST_3, ST_5, ST_7. The subscript denotes the number of grams of CNT used per 100 gm of rubber.

Table 2 Designation and formulation details of SBR-MWCNT Nanocomposites (Parts per Hundred of Rubber)

Designation	SBR rubber	Sulphur	Zinc Oxide	Stearic acid	TMTD	MBTS	MWCNT
ST_0	100	1.5	5	2	1.2	1.6	0
$ST_{0.5}$	100	1.5	5	2	1.2	1.6	0.5
ST_1	100	1.5	5	2	1.2	1.6	1
ST_3	100	1.5	5	2	1.2	1.6	3
ST_5	100	1.5	5	2	1.2	1.6	5
ST_7	100	1.5	5	2	1.2	1.6	7

2.3 Nanocomposite characterizations

2.3.1 Morphological analysis

The morphology of the composites was analysed by TEM (JEM-2100HRTEM). The cryocut specimens prepared using an ultra-microtome (Leica, Ultra cut UCT) were placed on a 300 mesh Cu grids (35 mm diameter) and were analysed. The transmission electron microscope was operated at an accelerating voltage of 200 kV.

2.3.2 Diffusion experiments

Circular samples were cut from the vulcanized sheets using a sharp-edged steel die. Thickness of the sample was measured at several points using a screw gauge. These circular samples were weighed and then dipped in 30 ml of solvent taken in diffusion bottles. Samples were taken out of the bottles at constant time interval and the adhering solvent was blotted off from the surface gently and then immediately weighed on highly sensitive electronic balance. Weighed samples were immediately immersed into test bottle. The weighing was continued until equilibrium swelling was obtained. In order to avoid the error due to the evaporation of the solvent weighing must be completed within 30 seconds. Transport properties were studied at 4 different temperature namely 28^0C, 40^0C, 50^0C, 60^0C using toluene.

3. Results and Discussion

Diffusion of solvents through different nanocomposites was determined. Mole % uptake is determined using the formula

$$Q_t mol\% = \left(\frac{\left(Mass\ of\ solvent\ sorbed \Big/ Molar\ mass\ of\ solvent \right)}{Mass\ of\ polymer} \right) \times 100 \qquad \textbf{(1)}$$

The mole percentage uptake (% Q_t) for the solvent was plotted against the square root of time ($\sqrt{t}$). Diffusion of solvent through a composite depends on the geometry of the filler (size, shape, size distribution, concentration and orientation), properties of the matrix and interaction between the matrix and filler.

Effect of filler loading

Figure 1 shows the sorption curves of toluene through SBR- CNT nanocomposites at different CNT loading. It is observed that the swelling continues with a reasonable high rate of solvent uptake since the concentration gradient of the penetrant in composite is large. Then the rate of solvent uptake decreases due to reduced concentration gradient of the penetrant molecules. From the figure it is also clear that as the filler loading increases the equilibrium uptake decreases. Solvent uptake is minimum for ST_7 and maximum for ST_0. This can be explained based on the fact that local mobility of the polymer after vulcanization[17] gets restricted by reinforcement of nanoscale CNT due to strong filler−polymer interaction so the polymer chains become less flexible and this leads to low sorption behaviour. Another reason for decrease in solvent uptake for ST_7 sample is due to the good dispersion of CNT in the matrix. Here as the amount of CNT is increased its uniform distribution in the SBR matrix restricts the movement of solvent through it.

The good dispersion of the nano filler in the matrix increases the surface area of the reinforcing phase, which caused an excellent improvement in the solvent resistance characteristics of the nanocomposites.TEM images in Figure 2 support this. Generally, filler dispersion in polymer based composites is of great importance in governing their performance. At low concentration of CNT, amount of CNT is very low to form an extensive network structure and homogeneous distribution. So the solvent molecules can easily pass through the matrix. It can also be observed from Figures 2c and 2d that CNT particles are forming a local filler–filler network in the rubber matrix. As a result, transport of solvent molecules through the polymer is hindered. Diffusion of solvent molecules through the polymer membrane also depends on the free volume within the polymer matrix. With the addition of nano fillers free volume within the matrix decreases and hence equilibrium solvent uptake is diminished. Since the free volume of rubber is taken by the CNT, there is an increase in density values with increase in filler loading which is given in Table 3. The decrease in solvent uptake in the filled systems can also be explained in terms of the tortuosity of the path and the reduced transport area in polymeric membrane in the presence of fillers.

Table 3 Density values of SBR Composites

Sample designation	Density (gm cm^{-3})
ST_0	0.98
$ST_{0.5}$	0.98
ST_1	0.99
ST_3	1.00
ST_5	1.01
ST_7	1.02

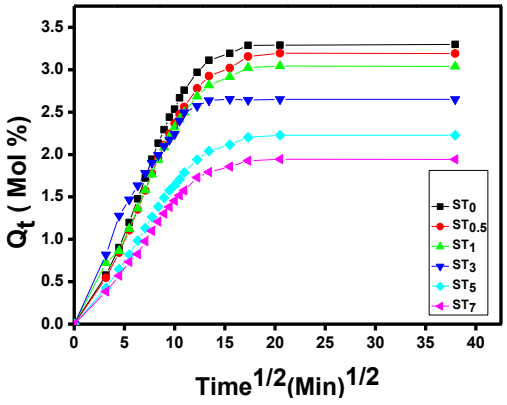

Fig. 1 Mole % toluene uptake of SBR composites with varying CNT loading.

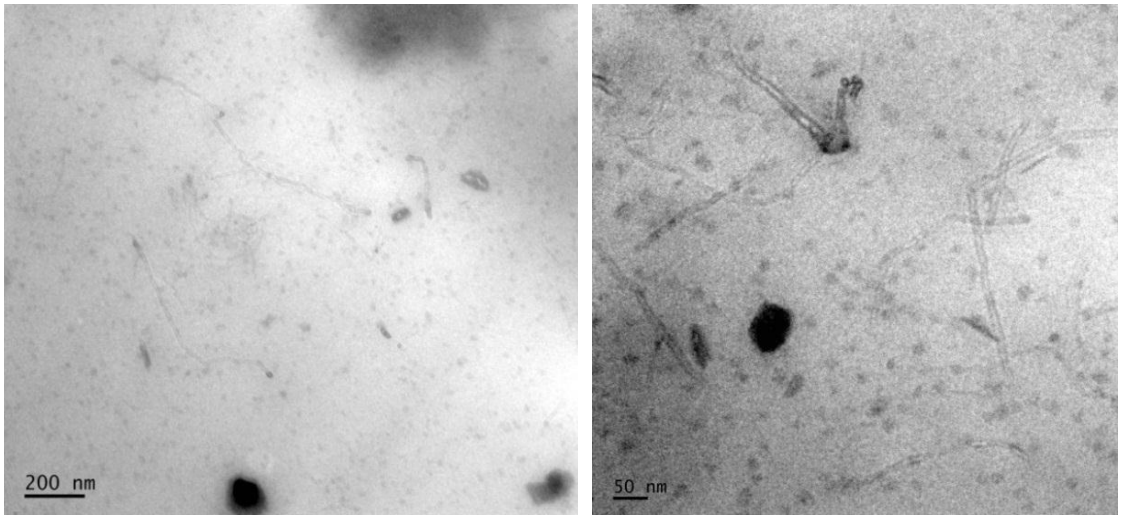

(a) (b)

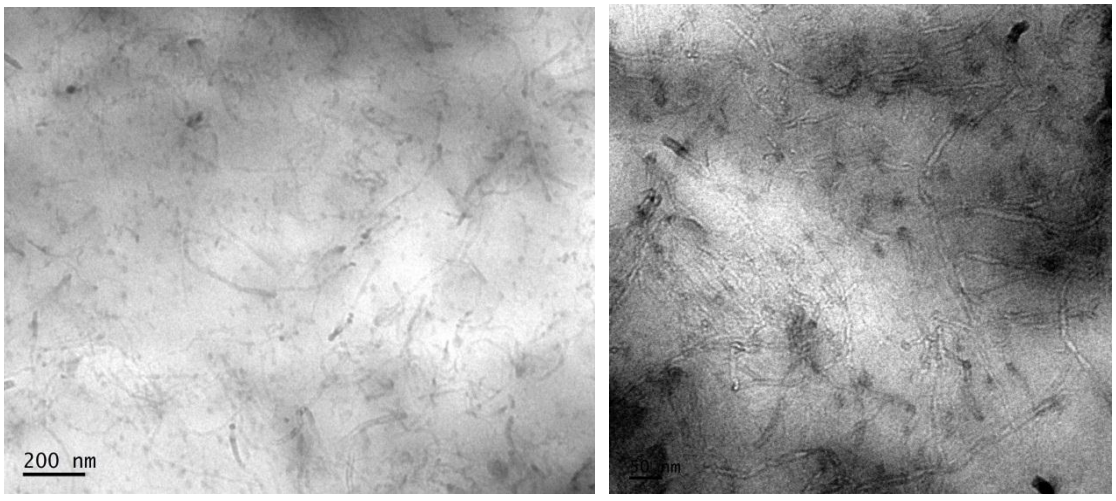

(c) (d)

Fig. 2 TEM Micrographs of ST_1 (a & b) ST_7 (c & d) composites.

Effect of nature of solvent

Homologue series of aromatic and aliphatic solvents were used to study the influence of penetrant size. Transport properties of composites in both aromatic and aliphatic solvents are investigated for ST_7 sample and these are shown in Fig. 3 and Fig. 4**.** A systematic trend for the diffusion of solvents through composites is observed. For aromatic solvents equilibrium uptake of xylene has found to be lower than that of toluene. The high molecular weight and molar volume of xylene might have effected in the lower equilibrium uptake.

The Q_∞ decreases with increase in molar volume and length of alkyl chains in the case of aliphatic solvents. The low solvent diffusion values of aliphatic solvents when compared to aromatic solvent are due to their high molar volume.[18] The decrease in diffusivity with increase in the size of the penetrant has been reported by many researchers.[19 20] This can be explained by free volume theory[21] according to which the diffusion rate of a molecule strongly depends on the ease with which the polymer chains exchange their positions with solvent molecules. As the penetrant size increases, the ease of exchange becomes less particularly in the case of filled matrices and this leads to a decrease in the solvent uptake. The high activation energy needed for large penetrant molecule is another reason for low solvent uptake.[22]

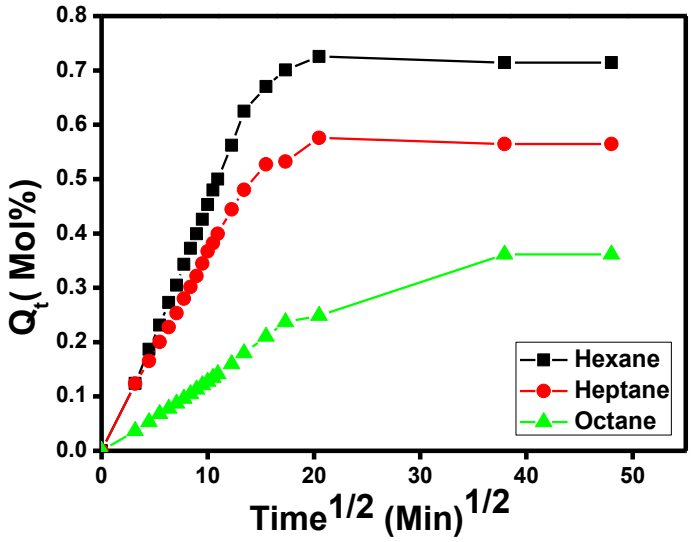

Fig. 3 Diffusion curves of ST_7 composites using aliphatic solvents

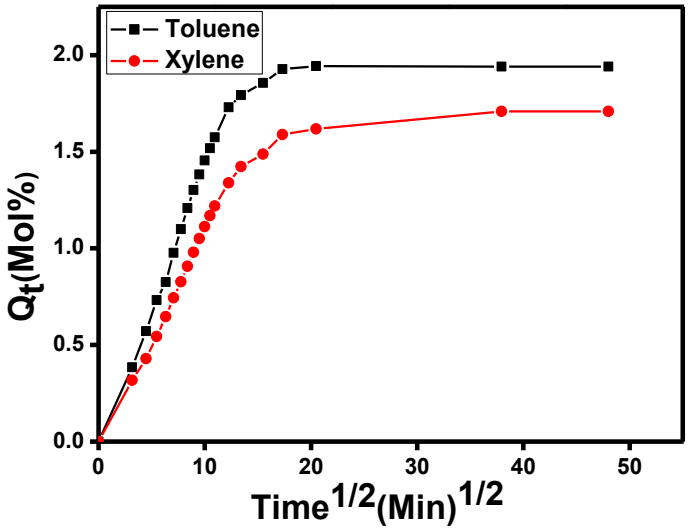

Fig. 4 Diffusion curves of ST_7 composites using aromatic solvents.

An attempt has been made to apply the Kraus[23] and Cunneen & Russel[24] equations to find the extent of reinforcement of fillers in the matrix.

According to Kraus equation

$$V_{r0}/V_{rf} = 1 - m\left(\frac{f}{1-f}\right) \qquad (2)$$

where V_{ro} and V_{rf} are the volume fraction of rubber in the solvent swollen rubber in the fully swollen unfilled sample and in the fully swollen filled sample respectively. f is the volume fraction of the filler and the slope m will be a direct measure of the reinforcing capacity of the filler in the elastomer matrix. V_{ro}/V_{rf} values of all the composition have calculated using toluene as the solvent and it was plotted against corresponding f/ (1 − f) values[Figure 5]. Reinforcing ability and swelling resistance caused by the filler is directly related. It can be also seen from the graph that V_{ro}/V_{rf} decreases with increase in CNT loading. The ratio V_{ro}/V_{rf} represents the degree of restriction of the swelling of the rubber matrix due to the presence of filler. So here ST_7 sample has better reinforcing ability due to its low V_{ro}/V_{rf} compared to other samples. According to the theory by Kraus, reinforcing fillers will have a higher negative slope. From the literature it is seen that when SBR is reinforced with different fillers like Cloisite 15A, Sepiolite clay and carbon nanofiber with slope of 2.55, 1.16 and 3.6 respectively. In present study the slope of 6.75 was obtained from Kraus plot, which indicates high reinforcing ability of CNT compared to other nano fillers.[25] This behaviour leads to a negative slope indicating the reinforcement effect of the CNT. Here better bonding between CNT and matrix represents a strong interface, which restricts the entry of solvent.

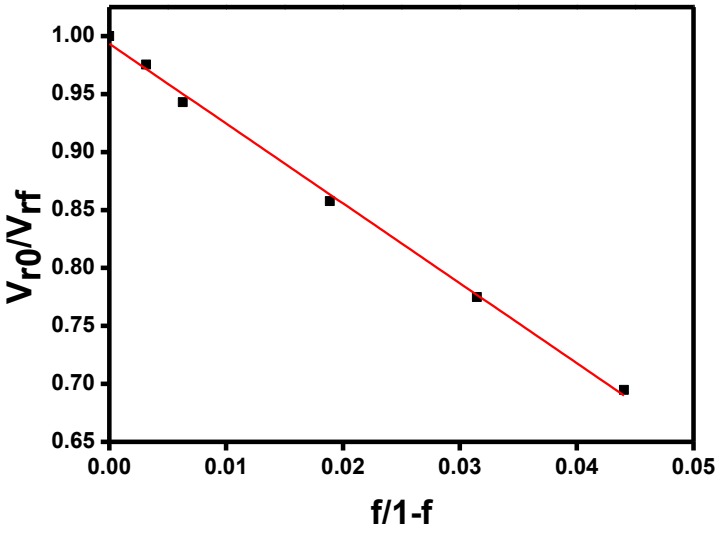

Fig. 5 Plot of V_{r0} /V_{rf} versus f/1 - f of SBR vulcanizates.

According to Cunneen and Russel equation,

$$V_{r0}/V_{rf} = ae^{-z} + b \qquad \textbf{(3)}$$

$V_{r0}$and V_{rf} have the same meaning as explained above, and *z* is the weight fraction of filler used. A plot of V_{r0} /V_{rf} versus e^{-z} should give a straight line with a slope that is a measure of the reinforcing ability of the filler. Both Kraus and Cunneen and Russel analysis support the high reinforcing nature of ST_7.

Sorption Behaviour

Mechanism of transport can be analysed by fitting dynamic swelling data in the equation[26]

$$\log Q_t/Q_\infty = \log k + n \log t \qquad \textbf{(4)}$$

where Q_t is the mole percent solvent uptake and k is a constant which depends on the structural characteristics and polymer/ solvent interaction, whereas the constant n gives the mode of sorption mechanism. The values of n and k are determined by power regression analysis of the linear portion of plots Q_t versus square root of time. If n = 0.5 mode of transport is Fickian, in which rate of diffusion of solvent molecules is lower than that of rate of relaxation of polymer chain.[27] n=1 indicates non- Fickian mode of transport, where chain relaxation is slower than the liquid penetration, while n between 0.5 and 1 indicates anomalous behaviour. When the solvent penetration is much below the polymer chain relaxation, it is possible to record the n values below 0.5. This situation is named 'Less Fickian.'Values of n and k obtained by regression analysis are compiled in Table 4.

Here *n* values are around 0.6 suggesting the deviation of transport mechanism from normal Fickian mode and hence can be classified as anomalous. Anomalous transport occurs due to the coupling of Fickian and non- Fickian behaviour. Variation from Fickian sorption is associated with the time taken by rubber segments to respond to swelling stress and rearrange them to accommodate the solvent molecules.[28] The reinforcement with the filler particle imparts a high degree of restriction to the

rearrangement of rubber chains. Slow viscous relaxation of polymer chain in the presence of carbon nanotube leads to anomalous transport behaviour. The *n* values tend to decrease with increase in the MWCNT content. This shows the better reinforcement effect at higher filler loading. The magnitude of k signifies the structural characteristics of the polymer and provides an idea about the nature of the interaction between the polymer and the solvent. The values of k in the filled systems are lower than the unfilled systems. This indicates that presence of filler can reduce the interaction between the polymer and the solvent. Among various composites value of k is lowest for ST_7 sample. This is due to the good dispersion of CNT in SBR matrix which results in poor solvent/ polymer interaction.

Table 4 Values of n and k for different CNT loadings in SBR composites using different solvents

	Solvent	n values						$kX10^{-2}$ values					
		ST_0	**$ST_{0.5}$**	**ST_1**	**ST_3**	**ST_5**	**ST_7**	**ST_0**	**$ST_{0.5}$**	**ST_1**	**ST_3**	**ST_5**	**ST_7**
Aliphatic	Hexane	0.61	0.58	0.60	0.57	0.57	0.55	1.39	1.31	1.39	1.33	1.26	1.20
	Heptane	0.65	0.58	0.62	0.62	0.55	0.50	1.52	1.36	1.44	1.43	1.37	1.13
	Octane	0.63	0.57	0.56	0.58	0.55	0.54	1.84	1.64	1.59	1.61	1.57	1.53
Aromatic	Toluene	0.64	0.63	0.54	0.59	0.58	0.57	1.38	1.37	1.21	1.25	1.29	1.06
	Xylene	0.66	0.66	0.65	0.62	0.59	0.56	1.53	1.47	1.48	1.41	1.44	1.31

.

Diffusion coefficient (D), Sorption coefficient (S), Permeation coefficient (P)

The diffusion coefficient (D) is a kinetic parameter which depends on the polymer segmental mobility and gives an indication of the rate at which a diffusion process takes place. It is the rate of transfer of the diffusing substance across unit area of cross section divided by the space gradient of concentration. Diffusion coefficient can be calculated using the formula which is obtained from second Fickian law.[29]

$$D = \left(h\theta / 4Q_{\infty} \right)^2 \qquad \textbf{(5)}$$

where h is the thickness of the sample, θ is slope of the linear portion of the graph Q_t versus $t^{1/2}$

As the CNT loading increases diffusion coefficient decreases due to the reduction in free volume with the addition of fillers. Another reason for decrease in diffusivity with increasing filler loading is due to the better dispersion of CNT in the matrix and also due to the better filler - polymer interaction which is confirmed from the TEM images given in Figure 2. Here there is secondary interaction between CNT and SBR. Phenyl ring on the SBR interacts with π electronic surface of CNT as shown Fig. 6. SBR is an amorphous polymer. But in its composite with CNT composites the amorphous region changes to rigid and mobile fractions. So when a nano particle is in corporate into polymer

matrix, three regions are generated. The aromatic styrene unit interacts with π electronic network of CNT by aromatic – π interaction and forms a rigid phase. The second region consists of polymer chains strongly bound to the rigid phase. The loose region (third region) is a zone loosely coupled to the second region. It has different chain structure and mobility and free volume compared to the polymer.[30] A hypothetical model indicating the rigid amorphous fraction is given in Figure 7. The thickness of this fraction will give clear indication about the filler matrix interaction. Diffusion coefficient values decrease with increase of penetrant size because of the high activation energy needed with increase in the size of the solvents. More over solubility parameter difference between rubber and the solvent plays an important role in the transport phenomena. Greater the difference lesser will be the diffusion coefficient. So aliphatic solvents show low D value compared to aromatic solvents. When we compare diffusion coefficients of ST_7 composites in different solvents it is observed that as the molar volume of the penetrant increases diffusivity decreases. Figure 8 shows the variation in diffusion coefficient with molar volume of the solvent.

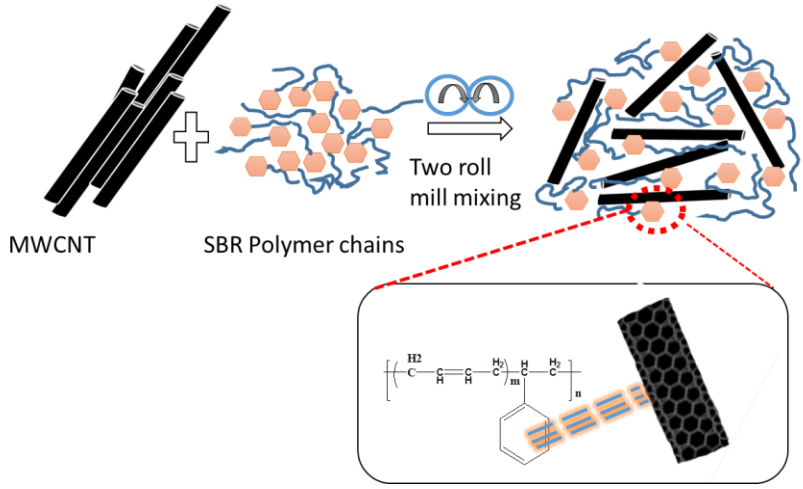

Fig. 6 Schematic representation of reinforcement effect of MWCNT in SBR matrix.

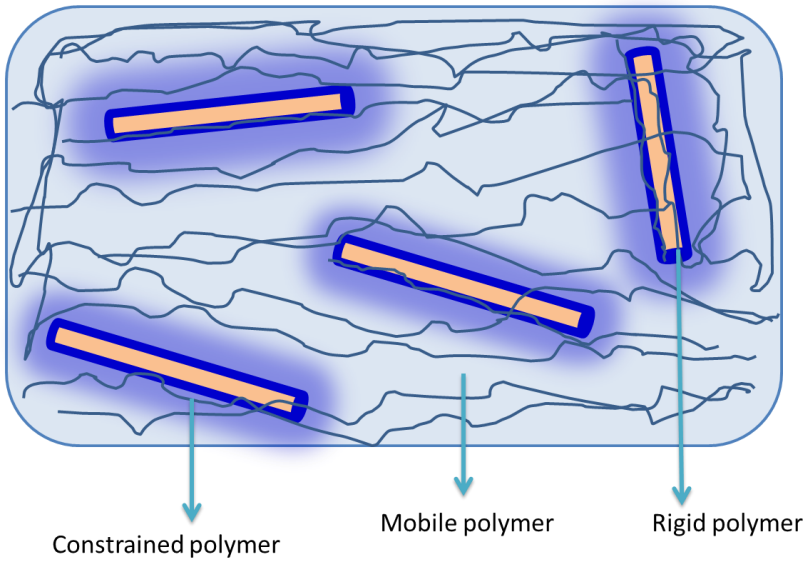

Fig. 7 Schematic representation of concept of Rigid Amorphous phase (RAF) in MWCNT filled SBR matrix.

The permeation of a penetrant into a polymer membrane depends on the diffusivity as well as on the sorption. Sorption coefficient is calculated using the equation $S = M_\infty/M_o$. The permeability coefficient (P) gives an idea about the amount of solvent permeated through uniform area of the sample per second. It is given by P = DS, permeation coefficient is the product of diffusion and sorption coefficient.[31] The variation in diffusion coefficient and permeation coefficient for the different CNT loadings at room temperature in toluene are shown in Figure 9. The diffusion coefficient generally decreases as the filler content increases. Lower value for diffusion coefficient indicates the low level of solvent permeation through polymer. From the Table 5 it is clear that ST_0 samples show maximum diffusivity and permeability in all solvents, whereas both are minimum for ST_7 sample.

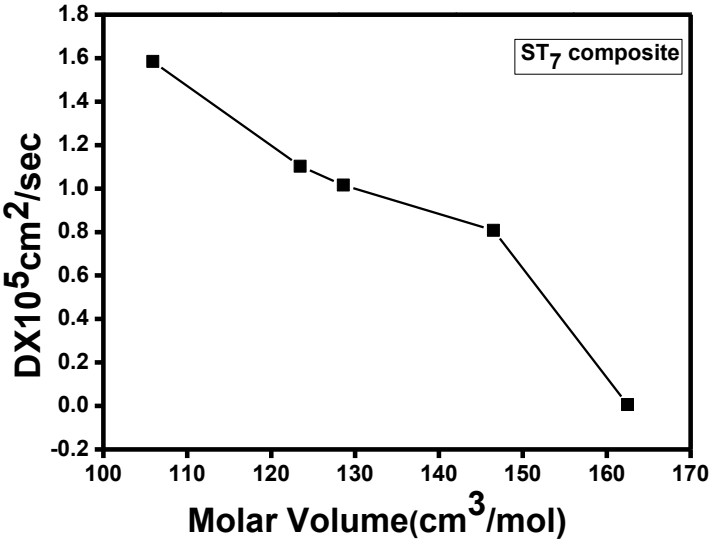

Fig. 8 Variation in Diffusion coefficient of ST_7 sample with molar volume of the solvent

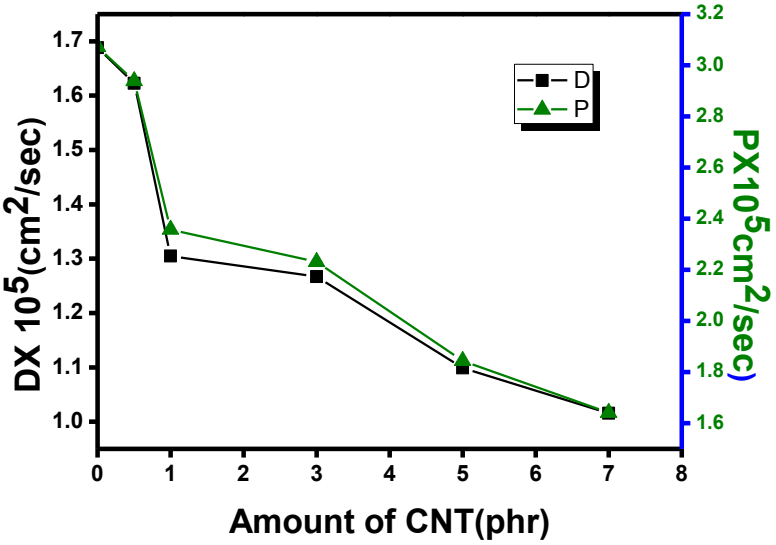

Fig. 9 Variation in D & P of composites with different CNT loading in toluene

Swelling parameters

Swelling studies give information on the interface strength, degree of dispersion of filler and their alignment in the elastomer matrix. In order to understand the extent of swelling behaviour of gum and filled vulcanizates swelling parameters like swelling index, swelling coefficient were evaluated. This gives a supporting evidence for the interfacial interaction between filler and the polymer.[32 33]

Swelling coefficient

Swelling coefficient is an index of the ability with which the sample swells.

$$Swelling\ \ Coefficent = \left[{(W_2 - W_1)}/{W_1} \right] \times \rho_s \qquad \textbf{(6)}$$

where W_1 and W_2 are the initial and final (swollen) weights of the sample and ρ_s is the density of solvent.

Swelling index

$$Swelling\ \ Coefficent = \left[{(W_2 - W_1)}/{W_1} \right] \times 100 \qquad \textbf{(7)}$$

Values of both swelling coefficient and swelling index were found to be decreasing with increasing filler content irrespective of the solvent used. The reason behind this is the hindrance in the path of solvent molecule with increased filler concentration. Sorption values also depend on the physicochemical properties of the penetrant such as molar volume of the solvent and length of the alkane chain of hydrocarbon. Here molar volume is in the order Hexane (128.61) < Heptane (146.50) < Octane (162.48). Normally as the molar volume of the solvent increases equilibrium swelling decreases due to the difficulty of long alkane chain to penetrate through the polymer. So for ST_0 sorption index (Table 4) is in the order Hexane>Heptane>Octane. This is truly due to molar volume effect.

Table 5 Values of Diffusion coefficient, Sorption coefficient, Permeation coefficient, Swelling coefficient and Swelling index for different composites in different solvents

Solvent	Sample	$Dx10^5 cm^2\ sec^{-1}$	Sorption coefficient	$Px10^5 cm^2\ sec^{-1}$	Swelling coefficient	Swelling index (%)
Hexane	ST_0	1.68	1.81	3.07	0.54	81.97
	$ST_{0.5}$	1.62	1.81	2.93	0.53	81.10
	ST_1	1.30	1.80	2.35	0.53	80.63
	ST_3	1.26	1.76	2.23	0.50	76.04
	ST_5	1.09	1.67	1.84	0.44	67.81

	ST_7	1.01	1.61	1.64	0.40	61.57
Heptane	ST_0	1.31	1.76	2.30	0.52	76.13
	$ST_{0.5}$	1.17	1.75	2.07	0.51	75.68
	ST_1	1.13	1.73	1.96	0.50	73.29
	ST_3	1.11	1.69	1.89	0.47	69.66
	ST_5	0.85	1.63	1.40	0.43	63.75
	ST_7	0.80	1.56	1.26	0.38	56.56
Octane	ST_0	0.02	1.52	0.032	0.36	52.31
	$ST_{0.5}$	0.015	1.52	0.022	0.36	52.18
	ST_1	0.014	1.51	0.021	0.36	51.49
	ST_3	0.013	1.49	0.020	0.34	49.78
	ST_5	0.008	1.46	0.012	0.32	46.05
	ST_7	0.005	1.41	0.008	0.29	41.29
Toluene	ST_0	2.26	4.03	9.16	2.63	303.80
	$ST_{0.5}$	1.80	3.93	7.12	2.54	293.91
	ST_1	1.67	3.80	6.36	2.42	280.10
	ST_3	1.66	3.44	5.71	2.11	244.17
	ST_5	1.61	3.05	4.94	1.77	205.26
	ST_7	1.58	2.78	4.42	1.55	178.84
Xylene	ST_0	1.88	3.86	7.28	2.46	286.41
	$ST_{0.5}$	1.71	3.80	6.53	2.41	280.54
	ST_1	1.51	3.66	5.53	2.29	266.81
	ST_3	1.50	3.41	5.12	2.07	241.76
	ST_5	1.35	3.05	4.57	1.76	205.07
	ST_7	1.10	2.81	3.10	1.56	181.48

Effect of temperature on transport phenomena

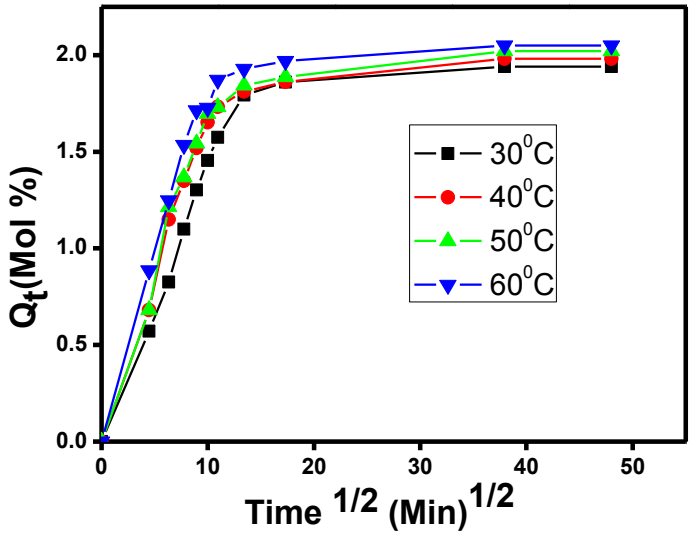

Fig. 10 Effect of temperature on transport phenomena of ST_7 composite.

In order to study the effect of temperature on transport properties, experiments are conducted at high temperatures such as 40^0C, 50^0C, 60^0C in addition to room temperature for ST_7 sample. Reason for selecting ST_7 sample for temperature study is due to its best solvent resistance at room temperature. Solvent used was toluene. Fig. 10 indicates that temperature has a significant effect on Q_∞ values. Q_∞ values at these temperatures show increased solvent uptake with increasing temperature. It is also found that the slope of the linear portion increases with temperature showing that the transport properties are temperature dependent. This can be attributed to the increase in free volume as a result of the increase in segmental motion of the polymer matrix as well as the gain in kinetic energy by the solvent molecules which resulted from the increased number of collisions at high temperature. So diffusion is a temperature dependent process. The D, S, and P values increased with increase of temperature and it is given in the Table 6.

Table 6 Values of D, S and P of ST_7 sample at different temperatures

Temperature (K)	$DX10^5$ cm^2/sec	S	$P X10^5$ cm^2/sec
301	1.58	2.79	4.42
313	1.59	2.83	4.52
323	1.63	2.86	4.68
333	1.71	2.89	4.96

The values of D and P at different temperatures were used to estimate the activation energy for diffusion using the Arrhenius relationship[34]

$$X = X_0 e^{-E/RT} \qquad \textbf{(8)}$$

where X is P or D and X_0 is P_0 or D_0 which is a constant. Activation energy plots of log D versus 1/T and log P versus 1/ T are shown in figure 11. From these plots, the activation energy needed for diffusion of toluene through the composites is calculated and is summarized in Table 7. From the difference between Ep and E_D, the heat of sorption, ΔH, was estimated. From Table 7 it is clear that activation energy for permeation and diffusion for filled composites is higher than that of unfilled composites.

Table 7 Arrhenius Parameters E_P, E_D, and ΔH ($KJmol^{-1}$) in toluene as the solvent

KJ mol^{-1}	ST_0	$ST_{0.5}$	ST_1	ST_3	ST_5	ST_7
E_P	5.22	6.27	7.15	5.37	2.55	3.12
E_D	4.53	5.518	6.32	3.78	1.58	2.21
Enthalpy Change (ΔH)	0.69	0.76	0.83	1.59	0.97	0.91

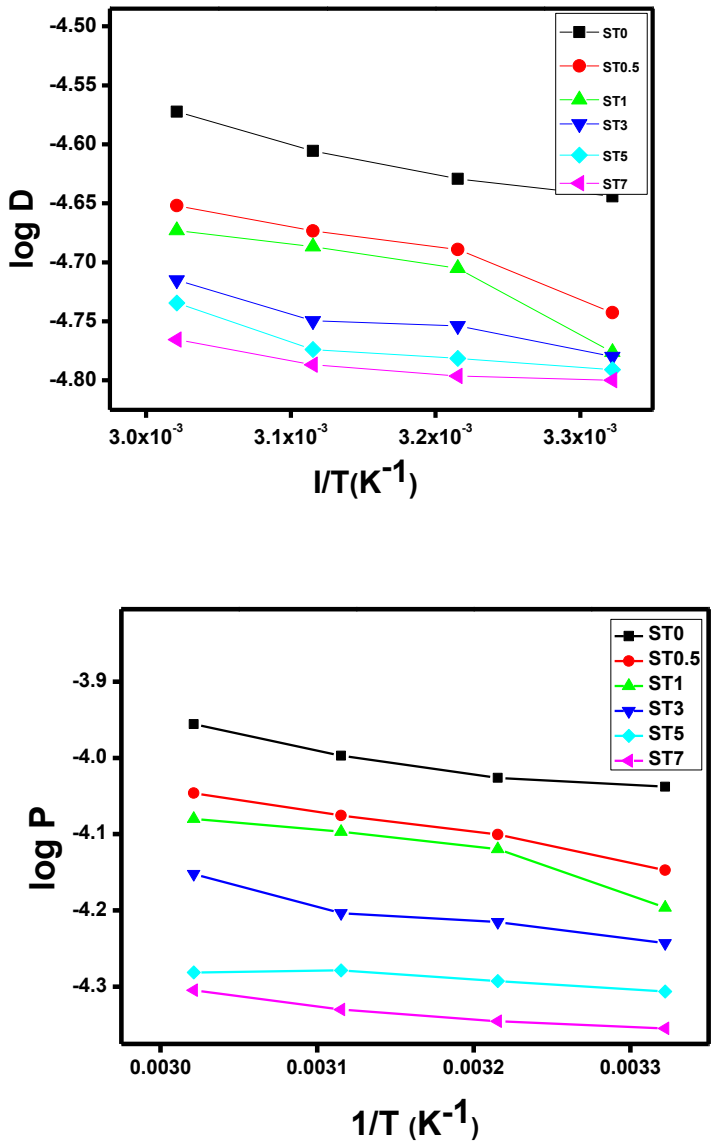

Fig. 11 Arrhenius plot of log D versus 1/T and log P versus 1/T.

Thermodynamic Parameters

The thermodynamic parameters for diffusion, ΔH^0 and ΔS^0 can be calculated using van't Hoffs relation.

$$Log\ Ks = \frac{\Delta S^0}{2.303R} - \frac{\Delta H^0}{2.303RT} \quad \textbf{(9)}$$

where, Ks is the equilibrium sorption constant, which is given by,

$$Ks = \frac{No.of\ \ moles\ \ of\ \ solvent\ sorbed\ at\ equllibrium}{Mass\ of\ \ polymer}$$

The values of $\Delta H^0$and ΔS^0 are obtained by the regression analysis of the plots of log Ks versus 1/T. The values of ΔH^0 and ΔS^0 are given in Table 8. It can be seen from the table that all the samples have positive ΔH^0 values which indicates the endothermic nature of sorption process. More over this process is governed by Henry's law according to which sorption proceed by the creation of new holes in the polymer. Change in entropy is positive for all samples and entropy decreases with increase in filler concentration. This is due to the increased number of filler polymer contacts at higher filler loading which reduces the solvent transport. The value of free energy is maximum for ST_0 sample and minimum for ST_7 sample. It can be understood that sorption process is more spontaneous for ST_0 sample and spontaneity of the reaction decreases with increasing filler loading. The value of ΔG becomes less negative with an increase in the percentage of CNT in the rubber matrix. These values indicate the increase in tortuosity of diffusion process through the matrix with an increase in the percentage of CNT in the elastomer matrix.

Table 8 Values of thermodynamic parameters of CNT-SBR composites with toluene as solvent

Sample	ΔH^0(KJ mol^{-1})	ΔS^0(KJ mol^{-1})	(-)ΔG^0(KJ mol^{-1})
ST_0	0.683	0.036	10.045
$ST_{0.5}$	0.750	0.033	9.263
ST_1	0.839	0.033	9.114
ST_3	1.597	0.033	8.267
ST_5	1.11	0.032	8.486
ST_7	1.028	0.031	8.448

Kinetics of diffusion

The transport kinetics of solvent through SBR composites can be studied by applying first-order kinetic equation as given[35]

$$\log\left(C_\infty - C_t\right) = \log C_\infty - \frac{K_1 t}{2.303} \qquad \textbf{(10)}$$

Figure 12 represents the plot of log (C∞- Ct) versus t for different filler loadings. On analysing the nature of the plot it is clear that transport of solvent though polymer follows first order kinetics. From the slope of the plot we can calculate the rate constant of diffusion process. Rate constant obtained are tabulated in Table 9. Rate constant (K_1), represents the quantitative measure of the speed (ease) with which polymer uptake the solvent. As the filler loading increases rate of the swelling decreases and this is due to increased CNT rubber interaction at higher filler loading. Both polymer solvent interaction parameter (k from Table 4) and rate constant (K_1) decreased as the filler loading increases due to increased CNT Rubber interaction at higher filler loading.

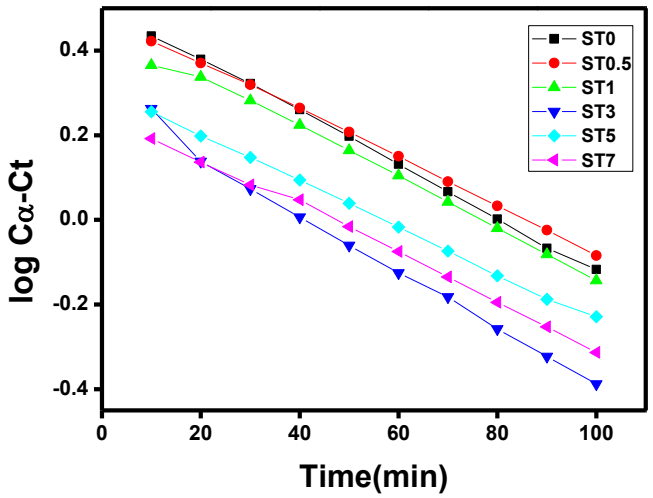

Fig. 12 Plot of log (C∞ - Ct) versus time for different nano composites in toluene at 301 K.

Table 9 Values of rate constant for SBR-CNT composites

K_1 X10^2min^{-1}	ST_0	$ST_{0.5}$	ST_1	ST_3	ST_5	ST_7
Rate constant	1.44	1.30	1.27	1.24	1.23	1.12

Network structure analysis

Molecular mass between successive cross links can be determined by Flory−Rehner equation[36]

$$Mc = -\frac{\left(\rho_r V_s \phi\right)}{\ln(1-\phi) + \phi + \chi\phi^2} \qquad \textbf{(11)}$$

where ρ_r is the density of rubber, Vs is the molar volume of the solvent, Ø is the volume fraction of the rubber in the swollen state. χ is solvent polymer interaction parameter. Ø is given by the Eq. (12) of Ellis and Welding[37]

$$\phi = \frac{\left(\frac{d - fw}{\rho_p}\right)}{\left(\frac{d - fw}{\rho_p}\right) + \frac{A_s}{\rho_s}} \quad \textbf{(12)}$$

where d is the deswollen weight of the polymer, f is the volume fraction of the filler, w is the initial weight of the polymer, A_s is amount of solvent absorbed. Solvent polymer interaction parameter χ is determined using Hildebrand Equation[38]

$$\chi = \beta + \frac{V_s(\delta_s - \delta_p)^2}{RT} \quad \textbf{(13)}$$

where β is the lattice constant, V_s is the molar volume, R is the universal gas constant, T is the absolute temperature, δ_s and δ_p are solubility parameter of the solvent and polymer respectively. The cross-link density can be determined from equation

$$Crosslinkdensity\ \upsilon = {}^{1}\!/_{2M_c} \quad \textbf{(14)}$$

Values of molecular mass (M_c) and cross link density (υ) are given in Table10. From the table it is clear that M_c value is maximum for ST_0which indicates that maximum solvent uptake is for ST_0. M_c value decreases from ST_0 to ST_7, so samples have different cross link density. As the filler loading increase value of M_c decreases this means filler polymer interaction increases with filler loading and hence maximum solvent uptake decreases. ST_0 has the highest vale for M_c, so cross links are far away from each other and hence the maximum solvent uptake for ST_0. Comparatively prominent solvent uptake of aromatic solvents compared to aliphatic solvents can be explained by the large difference in their solubility parameter and low molar volume.

Table 10 Values of molecular mass (M_c) and cross link density (υ) for samples

solvent	Molecular mass(gm mol^{-1})					
	ST_0	$ST_{0.5}$	ST_1	ST_3	ST_5	ST_7
Hexane	716.52	704.64	688.88	650.80	618.26	529.92
Heptane	759.21	751.23	750.34	707.49	696.15	626.88
Toluene	2082.29	1990.87	1867.91	1566.34	1289.77	1042.40
Xylene	2159.67	2047.15	1951.08	1617.53	1345.27	1120.54

Solvent	Crosslink density(mol cc^{-1})					
	ST_0	$ST_{0.5}$	ST_1	ST_3	ST_5	ST_7
Hexane	0.6978	0.709	0.725	0.768	0.808	0.943
Heptane	0.658	0.665	0.666	0.706	0.718	0.797
Toluene	0.240	0.250	0.267	0.319	0.387	0.479
Xylene	0.231	0.244	0.256	0.309	0.371	0.446

To compare with the theory, the molecular weight between the cross links was compared with the affine limit of the model Mc(aff) and the phantom network model given by James and Guth.[39 40] The study of deformation of polymeric networks during the transport of molecules through the polymer, gives us a better understanding of the transport phenomena. The molecular weight between the cross links for the affine limit of the model [Mc (aff)] was calculated using the equation

$$Mc(aff) = \frac{\rho_p V \phi_{2m}^{2/3} \phi_{2m}^{1/3} \left(1 - \frac{\mu}{\vartheta \phi_{2m}^{1/3}}\right)}{-\left[\ln(1-\phi_{2m}) + \phi_{2m} + \chi \phi_{2m}^{2}\right]} \quad \textbf{(15)}$$

where μ and υ are the number of effective chains and junctions.[41] According to the phantom network model, the molecular weight between the cross links for the phantom limit of model Mc(ph) was calculated by equation.

$$Mc\,(ph) = \frac{\left(1 - \frac{2}{\chi}\right) \rho_p V \phi_{2c}^{2/3} \phi_{2m}^{1/3}}{-\left[\ln(1-\phi) + \phi_{2m} + \chi \phi_{2m}^{2}\right]} \quad \textbf{(16)}$$

where χ is polymer solvent interaction parameter and it is determined using Hildbrand and Scott equation[42] Calculated M_c values along with experimental values are given in Table 11.

Table 11 Values of M_c (ph).and M_c (aff).in g cm^{-3}

M_c (ph)						
Hexane	691.5	688.55	678.56	619.52	583.73	496.29
Heptane	732.70	725.01	722.06	674.30	652.77	592.41
Toluene	2010.28	1917.18	1795.09	1492.89	1219.2	980.40
Xylene	2084.28	1971.38	1875.02	1550.64	1271.70	1085.06
M_c (aff).						
Hexane	159.79	157.4	154.56	137.92	126.54	98.91
Heptane	169.71	163.74	162	148.00	134.98	126.80
Toluene	793.52	747.29	687.07	541.79	415.90	309.56
Xylene	802.94	748.2	701.38	554.88	422.08	326.37

It was found that the M_c values of phantom network model showed moderate agreement with the experimental values rather than with the affine model. Here the junction points fluctuate over time around their mean position without any hindrance from the neighbouring chain"

Comparison with theory

The main objective of mathematical modelling is to compare experimental values with theoretical predictions of diffusion behaviour and hence establish the mode of transport solvent molecules through polymer matrix. Here the Peppas– Sahlin equation was selected to predict the diffusion behaviour. According to this model diffusion in polymer matrices contains two processes, i.e. diffusion into the swollen polymer and matrix relaxation.[43]
According to Peppas– Sahlin

$$\frac{M_t}{M_\infty} = K_f t^m + K_r t^{2m} \qquad \textbf{(17)}$$

where $M_t/M\infty$ is the fraction of solvent released at time t, K_f is the diffusion Fickian contribution coefficient, K_r is the relaxation contribution coefficient and m is the purely Fickian diffusion exponent. When $K_f > K_r$ the release is mainly controlled by diffusion, when $K_r > K_f$, the diffusion is mostly due to matrix swelling. When $K_f = K_r$, the diffusion is a combination of diffusion and polymer relaxation.

Experimental data and Peppas– Sahlin model fitting values are plotted in Figure 13. From the figure it is clear that Peppas–Sahlin model fitted well for the experimental values, which is confirmed by the Correlation coefficient (R^2) values, the extent of fitting. This implies that the diffusion process is considered to be a combination of diffusion into the swollen polymer and the polymer relaxation process. The decrease in Kr value with increase in filler loading also shows restriction in polymer chain relaxation with an increase in filler polymer interaction [Table 12].

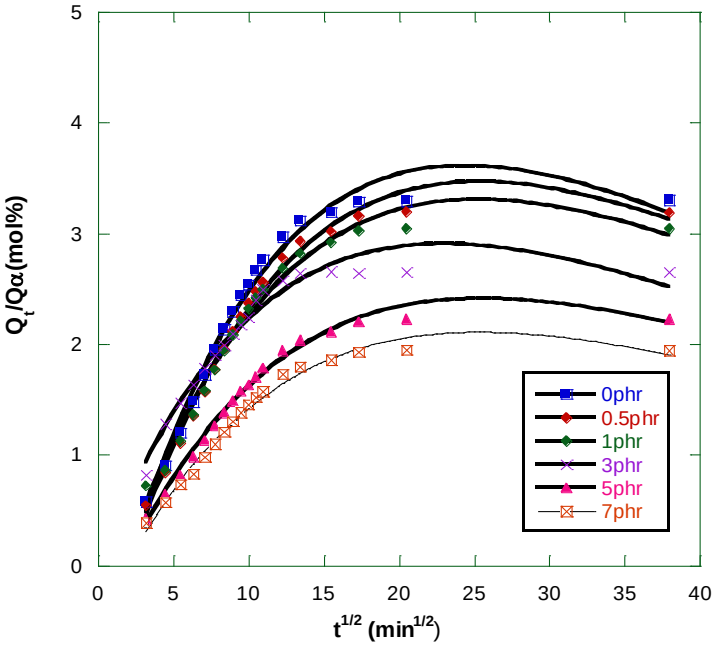

Fig. 13 Model fitting of the solvent permeation through SBR-CNT nanocomposites using Peppas–Sahlin

Table 12 Correlation coefficient (R^2) and constant (K_f & K_r) of Peppas– Sahlin fitting for different SBR vulcanizates.

	ST_0	$ST_{0.5}$	ST_1	ST_3	ST_5	ST_7
K_f	15.372	14.743	13.883	11.668	10.170	8.9111
K_r	-16.364	-15.679	-14.579	-11.175	-10.720	-9.406
R^2	0.9922	0.9945	0.9917	0.9834	0.9955	0.9934

Conclusion

The effect of CNT concentration on the transport behaviour of SBR composites is investigated. It is found that CNT concentration inversely influences the solvent uptake. The contributing factors to the improved solvent resistance of SBR- CNT nanocomposites can be summarized as (a) filler network formation leading to an efficient reinforcement, (b) proper dispersion of nanofillers in SBR matrix (c) formation of rigid polymer phase in the vicinity of CNT by the extended phenyl- π interaction (d) restriction in local mobility of polymer chains inside the filler networks. From the sorption curves it is concluded that as the size of the penetrant increases equilibrium uptake decreases which may be due to the high activation energy needed for large penetrant molecule. Here an anomalous transport occurs due to the coupling of Fickian and non- Fickian behaviour. Kraus and Cuneen Russel equation supports the high reinforcing ability of CNT. It was found that the temperature activates the diffusion process. The value of equilibrium mol% uptake also increases with the rise in temperature. The thermodynamic parameters for diffusion, ΔH^0 and ΔS^0 can be calculated using van't Hoffs relation. The transport kinetics of solvent through SBR composites can be studied by applying first-order kinetic equation. The molar mass between cross links was calculated using Flory−Rehner theory. The phantom and affine models were used to analyse the deformation of network during swelling. It was found that phantom models agree well with the experiment. The experimental diffusion results are in agreement with Peppas– Sahlin model which implies that the diffusion process is a combination of diffusion into swollen polymer and polymer relaxation process.

Acknowledgments

The authors would like to thank Council for Scientific and Industrial Research (CSIR), Delhi, DST Nanomission India for the financial support. Authors want to express their sincere thanks to Apollo Tyres Chennai for providing SBR.

References

[1] H. J. Barraza, F. Pompeo, E. A. O'rear and D.E. Resasco, *Nano Letters*, 2002, **2**, 797.
[2] M. D. Frogley, D. Ravich and H. D. Wagner, *Compos. Sci. Technol*., 2003, **63**, 1647.
[3] M. A. Lo´pez-Manchado, J. Biagiotti, L. Valentini and J.M. Kenny *J. Appl. Polym. Sci*., 2004, **92**, 3394.
[4] S. Iijima, Nature, 1991, **354**, 56.
[5] S.C. George and S. Thomas, *Prog. Polym. Sci*, 2001, **26**, 985−1017.
[6] R. Stephen, S. Varghese, K. Joseph, Z. Oommen and S. Thomas, *J. Membr. Sci*., 2006, **282**, 162.
[7] A.E. Mathai, R.P. Singh and S. Thomas, *J. Membr. Sci*., 2002, **202**, 35.
[8] J. Wang and W. Wu, *Eur. Polym. J*., 2005, **41**, 1143.
[9] T. Johnson and S. Thomas, *J. Mater. Sci*., 1999, **34**, 3221.

[10] G. Unnikrishnan and S. Thomas, *Polymer*, 1994, **35**, 5504.
[11] S.C. George, S.Thomas and K. N. Ninan, *Polymer*, 1996, **37**, 5839.
[12] S. C. George and S. Thomas. *J. Macromol, Sci, Phys b*, 2000, **39(2)**, 175–195.
[13] P.C. Thomas, J.E. Tomlal, P.T. Selvin, S.Thomas and K. Joseph, *Polym. Compos*., 2010 **31**, 1515–1524.
[14] O Starkova, S.T. Buschhorn, E. Mannov, K. Schulte and A. Aniskevich, *Eur. Polym. J*., 2013, **49**, 2138–2148.
[15] H.J. Maria, N. Lyczko, A. Nzihou, C. Mathew, S.C. George, K. Joseph and S.Thomas, *J. Mater. Sci*., 2013, **48**, 5373–5386.
[16] J. P. Jose and S. Thomas, *Phys. Chem. Chem. Phys*., 2014, **16**, 20190—20201.
[17] F.W. Billmeyer, Text book of polymer science. Wiley Interscience, Singapore. 1994
[18] M.S. Seehra, M. Yalamanchi and V. Singh, *Polym. Testing*, 2012, **4**, 564–571.
[19] L. M. Lucht and N.A. Peppas, *J. Appl. Polym. Sci*., 1987, **33**, 1557−1566.
[20] T. M. Aminabhavi and R.S. Khinnavar, Polymer, 1993, **34**, 1006−1018.
[21] R. Stephen, K. Joseph, Z. Oommen and S. Thomas, *Compos. Sci. Technol*., 2007, **67**, 1187−1194.
[22] G. Unnikrishnan and S. Thomas, *J. Appl. Polym. Sci*., 1996, **60**, 963-970.
[23] G. Kraus, *J. Appl. Polym. Sci*., 1963, **7**, 861.
[24] J. I. Cunneen and R.M. Russell, *Rubber Chem. Technol*., 1970, **43**, 1215.
[25] M Bhattacharya and A.K Bhowmick, Polymer, 2008, **49**, 4808-4818
[26] E. Southern and A.G. Thomas, *Trans. Farad. Soc*.,1967, **63**, 1913−1921.
[27] J. Wang, W. Wu and Z. Lin, *J. Appl. Polym. Sci*., 2008, **109**, 3018–3023.
[28] R.M. Barrer, J. A. Barrie and M. G. Rogers, *J. Polym. Sci. Part A*, 1963, **8**, 2565–2586.
[29] T. M. Aminabhavi and H. T. S. Phayde, *Polymer*, 1995, **36**, 1023.
[30] P.V. Thomas, S. Thomas, Sri Bandyopadhyay, A. Wurm and C. Schick *Compos. Sci. Technol*., 2008, **68**, 3220–3229.
[31] S.B. Harogoppad and T. M. Aminabhavi, *Macromolecules*, 1991, **24**, 2598.
[32] L. Mathew, K.U. Joseph and R. Joseph, *Bull. Mater. Sci*., 2006, **29**, 91–99.
[33] K.C. Manoj, P. Kumari, C. Rajesh, G. Unnikrishnan, *J. Polym. Res*., 2010, **17**, 1–9.
[34] A.E. Mathai and S. Thomas, *J. Macromol. Sci B Phys.*, 1996, **35**, 229−253.
[35] N. L. Thomas and A. H. Windle, *Polymer*, 1977, **18**, 1195.
[36] P. J. Flory and J. Rehner, *J. Chem. Phys.*, 1943, **11**, 512−521.
[37] B. Ellis and G.N. Welding, *Rubber Chem. Technol.*, 1963, **36**, 562
[38] C. H. M. Jacques and H.B. Hopfenberg, *Polym. Eng. Sci.*, 1974, **14**, 441–448.
[39] P. J. Flory Principles of polymer chemistry. Cornell University Press, Ithaca, 1953.
[40] L. R. G. Treloar The physics of rubber elasticity. Clarendon Press, Oxford, 1975.
[41] J. E. Mark and B . Erman Rubber Like Elasticity-A Molecular Approach; Wiley Inter Science: New York, 1988.
[42] Cowie JMG (1991) Polymers: chemistry and physics of modern. Chapman and Hall, New York
[43] N. A. Peppas and J. J. Sahlin, *Int. J. Pharm.*, 1989, **57**, 169–172.